Deep Learning Model for Endometrium Segmentation in Transvaginal Ultrasound (TVUS) Images

[1]Qurratu'Aini Thaqifah Ithani, [1]Siti Salasiah Mokri, [1]Noraishikin Zulkarnain, [2]Mohd Faizal Bin Ahmad

[1] *Dept of Electrical, Electronic and Systems Engineering, Universiti Kebangsaan Malaysia (UKM), Selangor, Malaysia*
[2] *Advanced Reproductive Centre (ARC) Hospital Canselor Tuanku Mukhriz (HCTM), Cheras, Malaysia*

siti1950@ukm.edu.my

Abstract. Manual analysis of endometrial thickness from transvaginal ultrasound (TVUS) images can lead to inconsistent interpretations due to varying expertise among medical professionals. Accurate endometrial thickness measurement is crucial for successful in vitro fertilization (IVF) treatments and increased pregnancy rates. Few studies have proposed deep-learning methods for endometrium segmentation in TVUS images, which are challenging due to their noisiness and blurriness. This study explores the application of a Transformer network for endometrium segmentation in TVUS images, aiming to leverage its ability to capture global context and long-range correlations. The dataset, collected from Hospital Canselor Tuanku Muhriz (HCTM), consists of 25 images, with 20 for training and 5 for testing. Images were pre-processed using MATLAB for cropping, removing text and symbols, masking, and resizing. Networks were trained using Python in Visual Studio Code with optimal parameters of 600 iterations, a batch size of 8, and a learning rate of 0.0001. Performance was evaluated using the dice coefficient. Results showed that U-Net outperformed the Transformer, achieving a dice coefficient of 0.977 compared to 0.956 on the test dataset. Despite a small difference of 2.20%, U-Net demonstrated better segmentation due to the limited training data, favoring its simpler architecture. Conversely, the Transformer network relies on global context and attention, requiring more data for effective feature extraction. Further research is needed to enhance the Transformer network's performance with small datasets.

Keywords: TVUS images, endometrium, Transformer, dice coefficient, segmentation.

1 Introduction

A worrying global trend of decreasing birth rates has been observed in recent years. Between 2007 and 2022, the number of births per 1,000 people worldwide fell dramatically, from 14.3 to 11.1, a decrease of over 23%. Malaysia is one of the countries whose fertility rates have fallen, from 6.7 per woman in 1957 to four in 1980, three in 2000, and 2.1 in 2010. The lowest rate in the history of the nation was reached

T. Amrillah et al. (eds.), *Proceedings of the International Conference on Advanced Technology and Multidiscipline (ICATAM 2024)*, Advances in Engineering Research 245,
https://doi.org/10.2991/978-94-6463-566-9_6

when it further decreased to 1.6 children per woman aged 15 to 49. The main contributing factor to these statistics is the infertility problem among trying couples. Infertility that results unsuccessful implantation and pregnancy may be affected by abnormal endometrial thickness.

The endometrium is the epithelial lining within the uterus, a pear-shaped organ housing the fetus along with its mucous membrane [1]. Hormonal changes during the menstrual cycle are intimately related to endometrial thickness (ET). The endometrial layer consists of several components, including blood cells, tissue spaces, glands, and skin cells. The thickening of the endometrium occurs during ovulation, preparing the wall of the fertilized egg for attachment. However, if fertilization does not occur, the endometrial lining sheds during menstruation. Abnormal changes in endometrial thickness serve as important signals of uterine illnesses.

A normal endometrium has no submucosal or myometrial abnormalities, is homogenous in echotexture, and has a consistent thickness [2] The occurrence of endometrial diseases is infrequent when the thickness of the endometrium is less than 5 mm. When ET is more than 8 mm in the proliferative phase or 16 mm in the secretory phase, the endometrium lining is abnormally thick which is also known as endometrial hyperplasia [3]. The risk of endometrial cancer is often increased when ET is > 3-5 mm, even though different studies have varied cutoff values. Examples of images of normal endometrium and endometrial hyperplasia condition are shown in Fig 1.

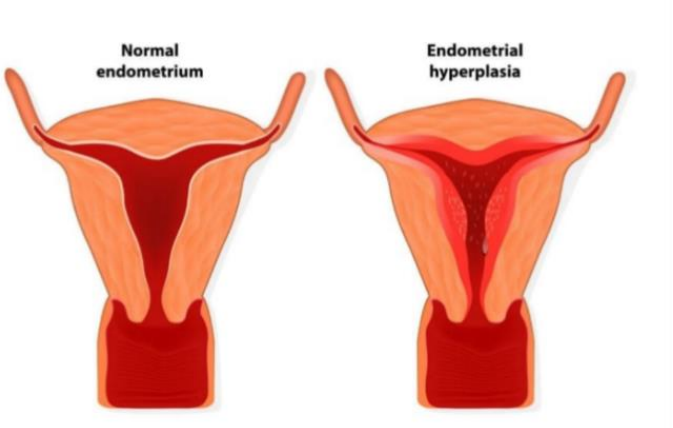

Fig. 1. Normal Endometrium and Endometrial Hyperplasia

Reproductive health such as endometrial issues and other fertility concerns are highly related to the number of populations. Malaysian couples who are facing the problem to conceive may consider treatment options such as In-Vitro Fertilization (IVF). Another alternative to IVF is in vitro oocyte maturation (IVM), which is also widely used worldwide to address fertility challenges [4]. A variety of factors are linked to male and female infertility, including physical conditions, lifestyle choices, genetic makeup, psychological issues, and hormonal disorders with unknown causes [5]. According to

the statistics, IVF contributes to 32% of pregnancies, in this method is suitable for patients with reproductive issues, such as irregular endometrium thickness. For this reason, Transvaginal ultrasonography (TVUS) imaging is the main screening technique utilized during the IVF procedure to monitor and assess the development of the ideal endometrial thickness for pregnancy [6]. This diagnostic procedure utilizes high-frequency sound waves that bounce off organs and tissues, allowing a computer to process the reflected sound waves and display clear scan images for analyzing internal organs. Consequently, it is essential to properly identify and characterize the endometrium during the TVUS scan. This study investigates the performance of a deep learning-based method to segment the endometrium in TVUS images. This task will pave the way for precise measurement of the endometrium thickness and better assessment of potential pregnancy by the experts.

2 Literature Review

Convolutional Neural Networks (CNNs) are a class of deep learning models that are highly utilized in computer vision, natural language processing, and image recognition. CNN has the advantage of learning features from large amounts of data [7]. Among others, some of CNN applications in medical image analysis are object detection, classification, and segmentation. CNNs are commonly proposed for image segmentation since they can recognize distinct picture parts using a variety of filters [8]. A CNN model consists of input layers, convolutional layers, activation functions, pooling layers, fully connected layers, and output layers. An image is fed into the network through the input layer, while high-level features are extracted by the convolutional, pooling, and activation layers[9]. After the objects are detected or classified by fully linked layers, the output layer produces the final predictions [10].

In 2015, Ronneberger, Fischer, and Brox developed U-Net, a machine-learning learning technique, designed specifically for image segmentation. For biomedical image segmentation tasks like detecting organs and cells in medical imaging, U-Net is highly advantageous. A "U-shaped" neural network is created using the U-Net design, which consists of an encoder for extracting features from pictures and a decoder to fix any mistakes [11]. The convolutional blocks in the encoder stage have several layers that increase the filter numbers while decreasing the size of the feature map. To recover the original size of the feature maps, the decoder section up-samples them and makes use of skip connections to preserve local information that is lost during downsampling. With this design, U-Net can segment medical pictures with high accuracy [12]. An example of U-Net architecture is shown below in Fig 2.

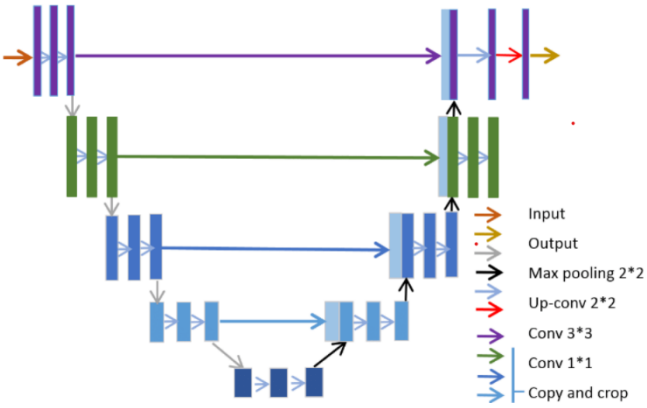

Fig. 2. U-Net architecture

In medical image segmentation, U-Net has been extensively utilized in previous research. Research from Jundi Wang [13] brought to light the need for segmentation approaches to identify tumour areas for diagnostic guidance. CNN-based techniques like U-Net to demonstrate efficient endometrial segmentation. Automated segmentation methods, such as U-Net, have been widely used for accurate data segmentation in medical imaging overcoming the weaknesses in manual segmentation [14]. Furthermore, other than segmentation, the deep learning method which is the Convolution Neural Network (CNN) also shows an outstanding performance in lung nodules classification [15].

Many factors are taken into consideration when measuring endometrial thickness, with an error range of ±2 mm which is regarded as clinically acceptable. Furthermore, the similarity between the actual and automated segmentation is measured using the dice coefficient. A 100% dice coefficient indicates perfect overlap between the predicted and actual labels. By integrating key-point discriminator technology into U-Net and FCN8 deep learning segmentation networks, Park et al. [16] achieved an 82.67% dice coefficient of segmentation accuracy. Hu et al. [17] on the other hand, used a VGG16-based U-Net for endometrial segmentation in TVUS images, employing a medial axis transformation technique to evaluate endometrial thickness. For each of the data sets, their analysis showed a dice score of 83% and mean absolute errors of 1.23 mm and 1.38 mm.

The majority of research in endometrium segmentation, utilizing both deep learning and conventional image segmentation methods, has been implemented on 2D images. However, Wang et al. [18] used U-Net to segment the endometrium in 85 3D transvaginal ultrasound (TVUS 3D) images and achieved a dice coefficient of 90.83%, which is 26.79% greater than that of 2D U-Net.

In continuation to this, this study investigates the performance of newly introduced Transformer networks and their comparison with Convolutional Neural Networks (CNN) to segment the endometrium in TVUS images. Thus far, the Transformer network has not been applied specifically for the segmentation of the endometrium in TVUS images. The novel architecture has the advantage of reducing overfitting and

handles easily long-range pixel dependencies while solving sequence-to-sequence tasks. Table 1 shows the overall comparison of previous studies related to U-Net segmentation.

Table 1. Comparison of previous studies related to U-Net segmentation

Previous studies	Method	Image number	Input image size	Dice (%)
Hu et al.	2D VGG-based U-Net	1,031	192x256	85.30
Park et al.	2D segmentation framework with a discriminator	3,372	256x320	82.67
Wang et. al	3D U-Net	2,480	224x224x32	90.83

3 Method

Fig 3 shows the methodology implemented in this study. The transformer neural network model represents an advancement in deep learning, particularly in the area of natural language processing (NLP). Its encoder-decoder design has an attention mechanism, which makes it efficient for tasks like paraphrasing phrases, text-to-speech synthesis, and voice recognition [19]. Two main parts make up the Transformer which are the encoder and the decoder. Each component comprises similar blocks, including layer normalization, masked multi-head attention modules, position-wise feed-forward networks, and multi-head attention modules. Output or predictions are based solely on prior outputs since the decoder's masked multi-head attention module focuses on the present position.

Shaohua Li et al. [20] developed Segtran, a Transformer-based segmentation system intended to improve computer-aided diagnosis through medical image segmentation. The final segmentation masks are produced by combining a CNN backbone for feature extraction with a Squeeze and Expansion Transformer for contextualization. Segtran overcomes the drawbacks of conventional frameworks such as U-Net, which performs well at collecting local characteristics but performs poorly in handling global context. Segtran is perfect for recording long-range correlations because it provides a broader receptive field even at high feature resolutions. Compared to DeepLabV3+ and U-Net, it has proven to perform better in a variety of medical picture segmentation tasks.

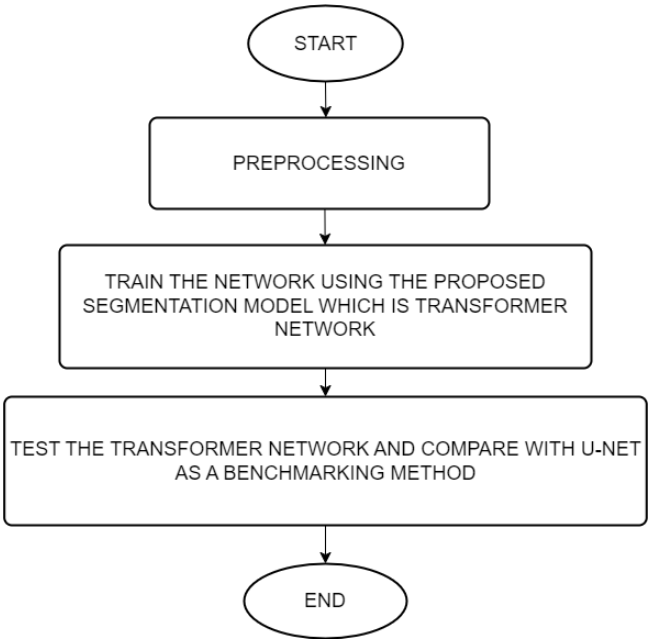

Fig. 3. Overall flowchart

This research utilizes Visual Studio Code with Python for endometrium segmentation in TVUS images. The following parameters are used:

- math for basic mathematical functions.
- numpy for scientific computing.
- torch for training neural networks.
- torch.nn for neural network layers.
- torch.nn.Parameter for learnable parameters.
- torch.nn.functional for mathematical operations.
- networks.segtran_shared for Segtran model configuration.
- train_util.batch_norm for batch normalization.
- efficientnet.model for efficient models.
- argparse.Namespace for command-line arguments.

3.1 Collect TVUS Images

In this study, the TVUS images were acquired from the Advanced Reproductive Center (ARC) of Hospital Canselor Tuanku Muhriz (HCTM), Malaysia. There are 25 endometrium TVUS images acquired out of 65 cases that include other cervical images. In addition, the ground truth of the endometrium boundaries was outlined by the radiologists of the ARC Center. Fig 4 below shows an example of a data set endometrium in TVUS images collected from ARC HCTM.

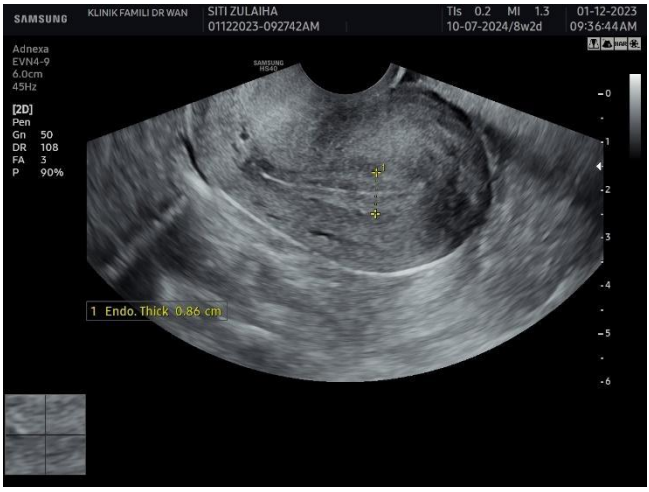

Fig. 4. Endometrium in TVUS images

3.2 Pre-processing images

The pre-processing process of the TVUS images was implemented using MATLAB. Firstly, every image was cropped to only highlight the endometrium region. To improve the dataset consistency and accuracy, any words and symbols found on the TVUS images were then eliminated using MATLAB Image Segmenter. Then, image masking was performed on the endometrium area by the radiologists from the ARC HCTM. In addition, each image was formatted to uint8 and resized to 576x576x3 pixels, which is the normal input image resolution for the Transformer network. A sample picture and mask image that are scaled to 576x576x3 in uint8 format are shown in Fig 5.

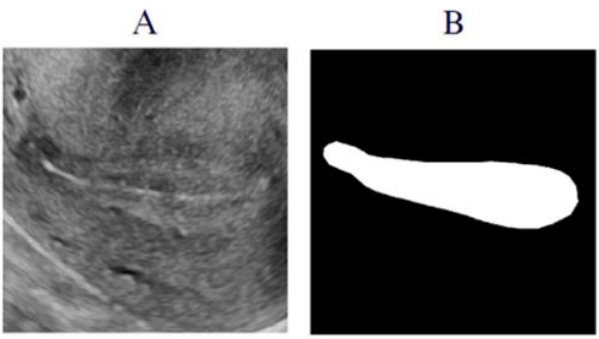

Fig 5. Actual images(A) and mask image (B) formatted to 576x576x3 in uint8 format

3.3 Train the Transformer network

The processed dataset was utilized for network training, along with an early stop to prevent overfitting and the optimization was based on the standard AdamW optimizer. Several values of learning rate were tested which are lr 0.0001, lr 0.001, lr 0.002, and lr 0.005. However, the 0.0001 learning rate showed the best segmentation results as the smaller learning rate supports better convergence and efficiently reduces the loss function. The dataset was divided into training (20) and testing (5), maintaining the ratio at 80:20. PyTorch was utilized to train the model.

3.4 Comparison of Transformer and U-Net

The trained network was tested with 600 iterations, as it yielded the best results as compared to 100, 150, 200, and 400 iterations. In general, segmentation performance and accuracy increase as the batch size increases. As bigger sizes resulted in memory problems, a maximum batch size of 8 was employed in this study due to system memory limits.

The performance of the segmentation accuracy is determined based on the dice similarity factor that compares the segmentation results using the Transformer and U-Net network with the ground truth as well as the validation loss. Both networks used the parameters of a learning rate of 0.0001, batch size of 8, and iteration of 600. The Dice Similarity Coefficient (DSC) is computed using the following formula.

$$DSC = \frac{2\,|G \cap P|}{|G| + |P|} \tag{1}$$

In image segmentation, binary cross-entropy (BCE) loss is commonly used [21]. BCE is calculated by comparing the predicted pixel vector to the actual pixel vector, as shown in the following formula. Here, yi represents the ground truth segmentation mask, and $\hat{y}$ is the predicted segmentation mask.

$$Loss_{BCE} \; - \sum_{i=1}^{N} \quad y_i \; log \; log \; (\hat{y}_i) \tag{2}$$

4 Result

4.1 Learning rate

In this study, the model was trained with a dataset of 20 images for training and 5 images for testing, using a learning rate of 0.0001, a batch size of 8, and 600 iterations. The training process showed excellent performance compared to higher learning rates. The dice coefficient for the Transformer and U-Net networks showed significant improvements, with scores of 0.956 and 0.977, respectively, at a learning rate of 0.0001. Fig 6 shows the graph of the Dice Coefficient versus the learning rate.

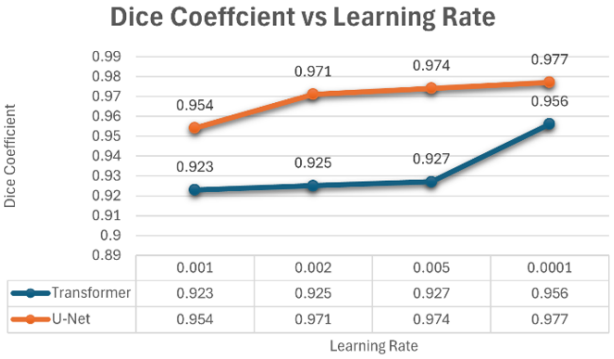

Fig. 6. The graph of the Dice Coefficient versus the learning rate

4.2 Iterations

The dataset of 20 training images and 5 testing images is used to train the model. A batch size of 4 and a learning rate of 0.0001 is set. Table 2 shows the results. This study tested various iterations to evaluate segmentation performance. At 600 iterations, U-Net achieved the highest dice coefficient of 0.966, while the Transformer reached 0.941. These results indicate that both models performed excellently, with U-Net slightly outperforming the Transformer.

Table 2. Iterations

Sample		Iteration	Batch size	Dice coefficient	
Train	Test			Transformer	U-Net
20	5	100	4	0.473	0.688
20	5	150	4	0.670	0.789
20	5	200	4	0.750	0.879
20	5	400	4	0.897	0.962
20	5	600	4	0.941	0.966

4.3 Batch Size

To measure segmentation performance depending on batch size, training began with a batch size of 2, 20 training images, 5 testing images, 600 iterations, and a learning rate of 0.0001. After testing several batch sizes, the study identified that the Transformer and U-Net performed best at batch sizes of 8, with a dice coefficient of 0.956 and 0.977, respectively. Memory capacity error arose with a batch size of 9. Overall, U-Net consistently performed better than Transformer which was probably because U-Net's simpler architecture performed better on the smaller dataset. Table 3 presents these findings.

Table 3. Batch Size

Sample		Iteration	Batch size	Dice coefficient	
Train	Test			Transformer	U-Net
20	5	600	2	0.868	0.933
20	5	600	4	0.941	0.954
20	5	600	6	0.943	0.966
20	5	600	8	0.956	0.977
20	5	600	9	CUDA out of memory	

4.4 Optimal Parameters

Various parameters, including the number of iterations, learning rate, and batch size, were tested to achieve the best model performance. Table 4 shows the optimal parameter configuration identified for the Transformer network, ensuring high accuracy and efficiency.

Table 4. Optimal Parameters

Parameter	Values
Iteration	600
Batch Size	8
Learning Rate	0.0001

4.5 Lost Function Graph for U-Net

Figs 7, 8, and 9 illustrate the cross-entropy (CE) loss, total training loss, and dice coefficient graphs for the U-Net model, respectively. These graphs show a steady

decline in losses throughout the training period. Initially, there were some fluctuations, but these reduced over time, resulting in smoother graphs. The loss values stabilized at relatively low levels, indicating successful convergence. U-Net efficiently captures local features in images and is less prone to overfitting compared to the Transformer model. This makes it more suitable for smaller datasets, where extracting important features from each image is essential.

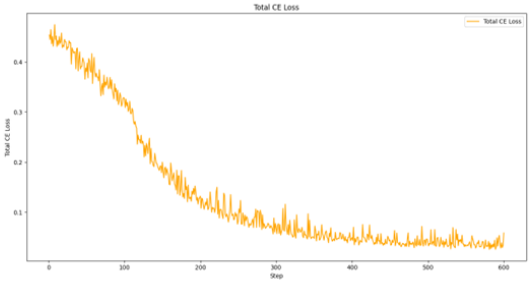

Fig. 7. Total CE loss for U-Net training

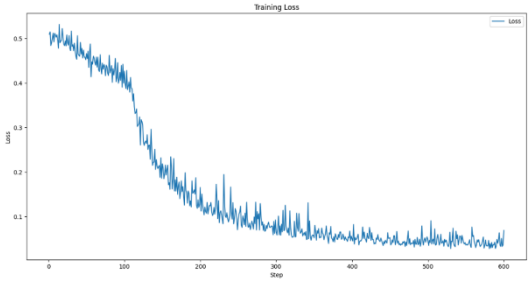

Fig 8. Training loss for I-Net training

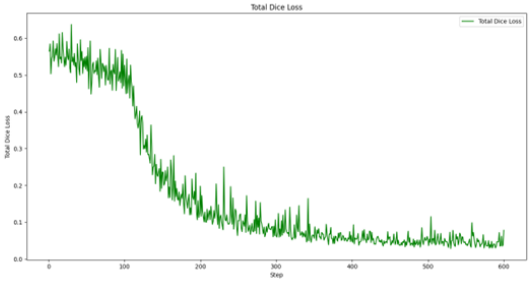

Fig. 9. Dice loss for U-Net training

4.6 Lost Function Graph for Transformer

The Transformer model cross-entropy (CE) loss, total training loss, and dice coefficient

graphs are shown in Fig 10, 11, and 12. When compared to U-Net, these graphs often show greater fluctuation throughout the training process. The transformer model experiences struggling convergence with high fluctuations considering its overall decreasing trend. The Transformer requires a bigger dataset for efficient training because it is a complex network architecture. It is prone to the problem of overfitting and has poor generalization towards a limited dataset. Additionally, a complicated model like the Transformer's training may not be stabilized with the same batch size of 8.

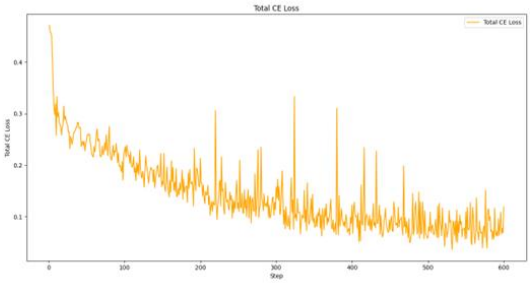

Fig. 10. Total CE loss for Transformer training

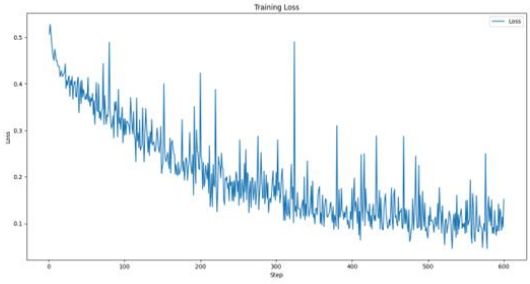

Fig. 11. Total Training loss for Transformer training

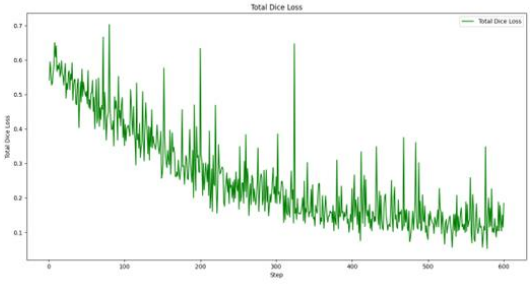

Fig. 12. Total Dice loss for Transformer training

4.7 Optimal Results

U-Net outperformed the Transformer with a dice coefficient of 0.977 compared to 0.956. U-Net is a simpler architecture and can handle small datasets more effectively, awarding its advantage over the Transformer, which requires larger datasets for optimal performance. Table 5 shows the optimal results for both networks.

Table 5. Optimal Results

Model	Dice Coefficient
Transformer	0.956
U-Net	0.977

5 Conclusion

This paper evaluates the performance of the Transformer network for segmenting endometrium in TVUS images in comparison to the well-established U-Net architecture. Experimental results show that U-Net outperforms the Transformer by 2.20% in the dice coefficient. Despite the small dataset, U-Net demonstrated excellent segmentation performance while the Transformer network performs less well when handling a limited dataset. Future research will focus on optimizing Transformer network capability to deal with small datasets considering its highly acclaimed advantage which is the ability to learn the long-range pixel dependency to obtain improved segmentation accuracy.

Acknowledgments. The authors would like to acknowledge the University Kebangsaan Malaysia and the Ministry of Education Malaysia (MOE) for the Research University Grant with code: GUP-2019-023 for the support of this project.

References

1. S. -Y. Hu, H. Xu, Q. Li, B. A. Telfer, L. J. Brattain and A. E. Samir,R. Nicole, “Deep Learning-Based Automatic Endometrium Segmentation and Thickness Measurement for 2D Transvaginal Ultrasound,” 2019 41st Annual International Conference of the IEEE Engineering in Medicine and Biology Society (EMBC), Berlin, Germany, 2019, pp. 993-997, doi: 10.1109/EMBC.2019.8856367.
2. J. Bansiya and C. G. Davis, "A hierarchical model for object-oriented design quality assessment," in IEEE Transactions on Software Engineering, vol. 28, no. 1, pp. 4-17, Jan. 2002, doi: 10.1109/32.979986.
3. Ahmad, M. F., Elias, M. H., Jin, N. M., Abu, M. A., Syafruddin, S. E., Zainuddin, A. A., Suzuki, N., & Karim, A. K. A. (2023). The spectrum of in vitro maturation in clinical practice: the current insight. Frontiers in Endocrinology, 14. https://doi.org/10.3389/fendo.2023.1192180
4. Karunyam, B. V., Karim, A. K. A., Mohamed, I. N., Ugusman, A., Mohamed, W. M. Y., Faizal, A. M., Abu, M. A., & Kumar, J. (2023). Infertility and cortisol: a systematic review. Frontiers in Endocrinology, 14. https://doi.org/10.3389/fendo.2023.1147306

5. Liu, Y., Zhou, Q., Peng, B., Jiang, J., Fang, L., Weng, W., Wang, W., Wang, S., & Zhu, X. (2022c). “Automatic measurement of endometrial thickness from transvaginal ultrasound images. Frontiers in Bioengineering and Biotechnology”, 10. https://doi.org/10.3389/fbioe.2022.853845
6. Kondagari, L., Kahn, J., & Singh, M. (2023, June 7). Sonography gynecology infertility assessment, protocols, and interpretation. StatPearls - NCBI Bookshelf. https://www.ncbi.nlm.nih.gov/books/NBK572093/
A. B. Nassif, I. Shahin, I. Attili, M. Azzeh and K. Shaalan, "Speech Recognition Using Deep Neural Networks: A Systematic Review," in IEEE Access, vol. 7, pp. 19143-19165, 2019, doi: 10.1109/ACCESS.2019.2896880.
7. Jabbar, S. Naseem, T. Mahmood, T. Saba, F. S. Alamri and A. Rehman, "Brain Tumor Detection and Multi-Grade Segmentation Through Hybrid Caps-VGGNet Model," in IEEE Access, vol. 11, pp. 72518-72536, 2023, doi: 10.1109/ACCESS.2023.3289224.
8. M. S. Azman, F. Rossi, N. Zulkarnain, S. S. Mokri, A. A. A. Rahni and N. F. Ali, "Classification of Lung Nodule CT Images Using GAN Variants and CNN," 2022 IEEE International Conference on Computing (ICOCO), Kota Kinabalu, Malaysia, 2022, pp. 310-315, doi: 10.1109/ICOCO56118.2022.10031756
9. Tandel, G. S., Biswas, M., Kakde, O. G., Tiwari, A., Suri, H. S., Turk, M., Laird, J., Asare, C., Ankrah, A. A., Khanna, N. N., Madhusudhan, B. K., Saba, L., & Suri, J. S. (2019). A review on a deep learning perspective in brain cancer classification. Cancers, 11(1), 111. https://doi.org/10.3390/cancers11010111
10. Ronneberger, O., Fischer, P., & Brox, T. (2015). U-NET: Convolutional Networks for Biomedical Image Segmentation. arXiv (Cornell University). https://doi.org/10.48550/arxiv.1505.04597
11. Ioffe, S., & Szegedy, C. (2015). Batch Normalization: Accelerating Deep Network Training by Reducing Internal Covariate Shift. ArXiv, abs/1502.03167.
12. J. Wang, L. Han and D. Ran, "Architectures and Applications of U-net in Medical Image Segmentation: A Review," 2023 9th International Symposium on System Security, Safety, and Reliability (ISSSR), Hangzhou, China, 2023, pp. 84-94, doi: 10.1109/ISSSR58837.2023.00022.
13. N. Siddique, S. Paheding, C. P. Elkin and V. Devabhaktuni, "U-Net and Its Variants for Medical Image Segmentation: A Review of Theory and Applications," in IEEE Access, vol. 9, pp. 82031-82057, 2021, doi: 10.1109/ACCESS.2021.3086020.
14. Mohd Isham, N. N., Mokri, S., Abd Rahni, A., & Ali, N. (2021). Classification of lung nodules in CT images using conditional generative adversarial – convolutional neural network. International Journal of Nonlinear Analysis and Applications, 12(Special Issue), 1047-1058. doi: 10.22075/ijnaa.2021.5551
15. Park, H., Lee, H. J., Kim, H. G., Ro, Y. M., Shin, D., Lee, S. R., Kim, S. H., & Kong, M. (2019b). Endometrium segmentation on transvaginal ultrasound image using key-point discriminator. Medical Physics on CD-ROM/Medical Physics, 46(9), 3974–3984. https://doi.org/10.1002/mp.13677
16. S. -Y. Hu, H. Xu, Q. Li, B. A. Telfer, L. J. Brattain and A. E. Samir, "Deep Learning-Based Automatic Endometrium Segmentation and Thickness Measurement for 2D Transvaginal Ultrasound," 2019 41st Annual International Conference of the IEEE Engineering in Medicine and Biology Society (EMBC), Berlin, Germany, 2019, pp. 993-997, doi: 10.1109/EMBC.2019.8856367.
17. Wang X, Bao N, Xin X, Tan J, Li H, Zhou S, Liu H. Automatic evaluation of endometrial receptivity in three-dimensional transvaginal ultrasound images based on 3D U-Net segmentation. Quant Imaging Med Surg. 2022 Aug;12(8):4095-4108. doi: 10.21037/qims-21-1155. PMID: 35919049; PMCID: PMC9338380.
18. Xiao, H., Li, L., Liu, Q., Zhu, X., & Zhang, Q. (2023). Transformers in medical image segmentation: A review. Biomedical Signal Processing and Control, 84, 104791. https://doi.org/10.1016/j.bspc.2023.104791
19. Li, S., Zhang, H., Ma, H., Feng, J., & Jiang, M. (2023). SSA NET: Small Scale-Aware Enhancement Network for Human Pose Estimation. Sensors, 23(17), 7299. https://doi.org/10.3390/s23177299
20. N. F. Ali, N. N. Md Nasry, I. Shah, S. S. Mokri and A. A. Abd Rahni, “Segmentation of Brain Glioma in MRI Images Using Deep Learning,” 2022 IEEE 20th Student Conference on Research and Development (SCOReD), Bangi, Malaysia, 2022, pp. 45-50, doi: 10.1109/SCOReD57082.2022.9973855.